iScience

CellPress
OPEN ACCESS

Article

Applying exercise-mimetic engineered skeletal muscle model to interrogate the adaptive response of irisin to mechanical force

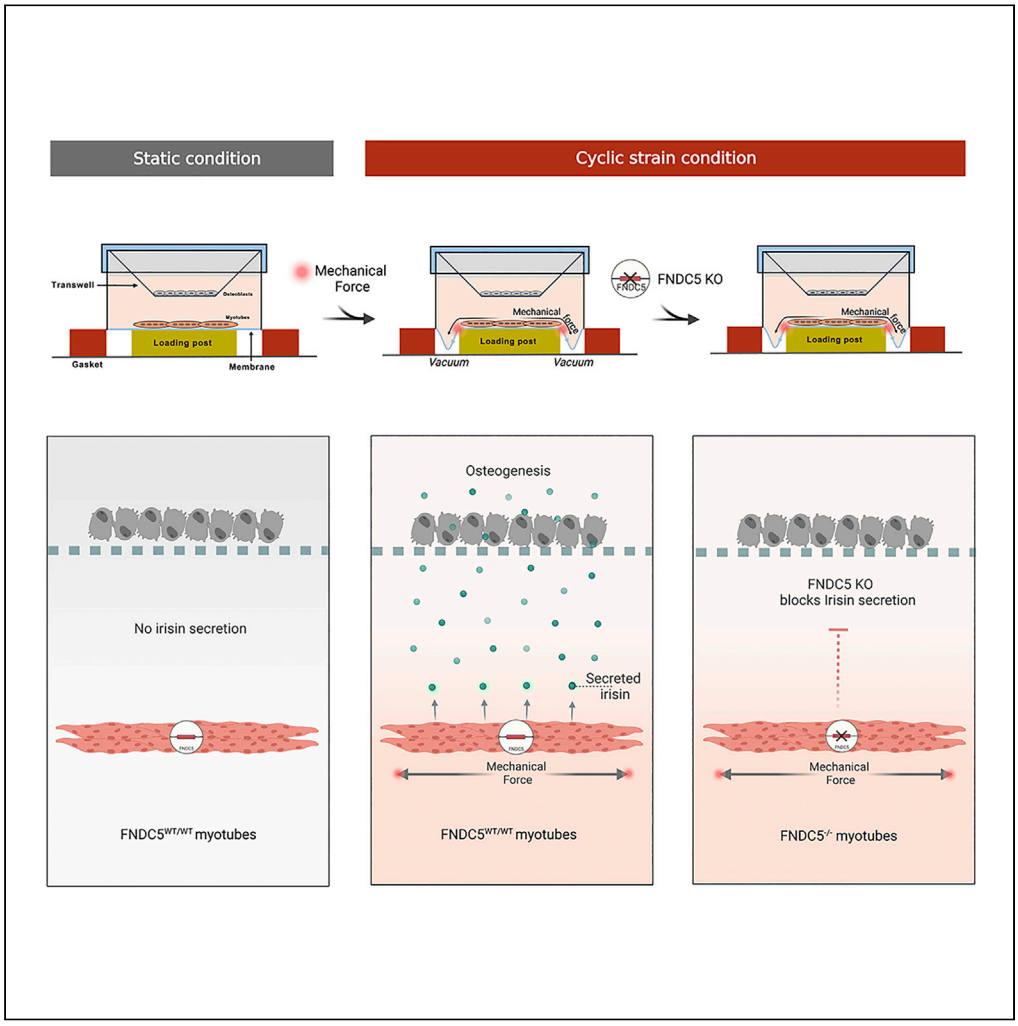

Yuwei Zhang, Lizhen Wang, Hongyan Kang, Chia-Ying Lin, Yubo Fan

lizhenwang@buaa.edu.cn (L.W.)
hongyankang@buaa.edu.cn (H.K.)

Highlights

Irisin is producible in an exercise-mimetic engineered skeletal muscle model

Enhanced irisin production in response to a long-term cyclic stretch

PGC-1α1 and PGC-1α4 mRNAs expression contributed to the generation of irisin

Demonstration that induced irisin in our model regulating osteoblasts as native ways

Zhang et al., iScience 25, 104135
April 15, 2022 © 2022 The Authors.
https://doi.org/10.1016/j.isci.2022.104135

iScience

CellPress
OPEN ACCESS

Article

Applying exercise-mimetic engineered skeletal muscle model to interrogate the adaptive response of irisin to mechanical force

Yuwei Zhang,[1] Lizhen Wang,[1,6,*] Hongyan Kang,[1,*] Chia-Ying Lin,[1,3,4,5] and Yubo Fan[1,2]

SUMMARY

Physical exercise induces the secretion of irisin from contractile muscle into circulation; however, the adaptive response of irisin to mechanical stimulus in skeletal muscle *in vitro* remains numerously unknown. In an effort to investigate whether irisin is inducible *in vitro*, we developed a bioreactor consisting of a retractable mechanical force controller and a conditional tissue culture system. Upon this model, a distinguished surge of irisin was detected in stretched myotubes as cyclic strain initiated, and the surge was able to be stalled by knocking out FNDC5. Intriguingly, increased irisin secretory is associated with the shifts of MyHC isoforms from anaerobic type to aerobic type in myotubes. We further revealed that PGC-1α1 and PGC-1α4 mRNAs expression, rather than PGC-1α2 and PGC-1α3, contributed to the generation of irisin in myotubes during cyclic strain. Lastly, combined with co-culturing MC3T3 osteoblasts, we demonstrated the bioactivity of generated irisin, promoting the osteogenic differentiation.

INTRODUCTION

Exercise has been well documented as a physical, rather than a drug treatment, to preclude and ameliorate several metabolic disorders including chronical disease including obesity, diabetes, and aging disease, for instance, muscular atrophy and osteoporosis (Booth et al., 2012; Cartee et al., 2016). In adult human body, about 40%–45% of mass is skeletal muscles which play an important role in generating movement or maintaining postures (Pedersen and Febbraio, 2012). Skeletal muscle is being passively stretched when encounters mechanical alteration and makes various biomechanical cascading reactions to adapt itself (Baar, 2006). These adaptive responses are able to advance myotube hypertrophy, oxidative ability, or endocrine capability, by means of, mostly, releasing myokines to extracellular and signal on other organs or tissues (Hoppeler et al., 2011; Rose and Hargreaves, 2003). However, illuminating the specific mechanism how myokines react to physical exercise or muscle contraction *in vivo* has been a challenge given the complicated constructure and interacting signaling network. Although some research exposed a small portion of it by conducting traditional assay like pathway analysis through relative genes of interest function gain or loss, as well as innovative approach such as mapping transcriptomic profile (Mahoney et al., 2005; Pillon et al., 2020).

Culture models and organoids *in vitro* would be an effective apparatus aiming to simplify and centralize versatile organism physiology and pathology on organ or tissue scales (Clevers, 2016). Engineered skeletal muscle has been extensively characterized as similar to those of primary muscle tissues during mechanical stimulation (Aas et al., 2013). *In vitro* myotubes, generated from fusion of precursor myoblasts and composed of multinucleated fibers, have been universally employed in researches to learn the function of skeletal muscle from molecular and cellular perspectives (Aguilar-Agon et al., 2019; Vandenburgh et al., 1989). Given their elastic properties, various studies have investigated the mechanoresponse of myotubes such as protein synthesis, hypertrophy, glucose uptake, and oxidative stress *in vitro* when they were subject to different mechanical alterations (Collinsworth et al., 2000; Gao and Carson, 2016; Moustogiannis et al., 2020; Vandenburgh, 1982; Vandenburgh et al., 1989). Evidence that demonstrating comparable adaptions of skeletal muscle in response to exercise training *in vivo* have also been well documented (Bodine et al., 2001; Hawley et al., 2014; Massart et al., 2021). Exceptionally, to date, limited skeletal muscle models have been established to integrally study exercise-induced myokine and its

[1]Key laboratory for Biomechanics and Mechanobiology of Ministry of Education, Beijing Advanced Innovation Centre for Biomedical Engineering, School of Biological Science and Medical Engineering, Beihang University, Beijing 100083, China

[2]School of Engineering Medicine, Beihang University, Beijing 100083, China

[3]Department of Biomedical, Chemical & Environmental Engineering, University of Cincinnati, Cincinnati, USA

[4]Department of Orthopaedic Surgery, University of Cincinnati, Cincinnati, USA

[5]Department of Neurosurgery, University of Cincinnati, Cincinnati, USA

[6]Lead contact

*Correspondence: lizhenwang@buaa.edu.cn (L.W.), hongyankang@buaa.edu.cn (H.K.)

https://doi.org/10.1016/j.isci.2022.104135

This is an open access article under the CC BY-NC-ND license (http://creativecommons.org/licenses/by-nc-nd/4.0/).

biological function on proximal tissues (Juffer et al., 2014; Yin et al., 2016). At our disposal in this regard, we established a bioreactor combing an advanced cyclic stretching system with a cultured muscle contraction model using well-characterized C2C12 myotubes.

In this study, here, we spotlighted on a myokine irisin, C-terminally cleaved multi-peptide fragments of the protein fibronectin type III domain-containing protein 5 (FNDC5), upregulated by peroxisome proliferator-activated receptor-γ coactivator (PGC1-α), releases and circulates in plasma as an adaptive response to exercise (Boström et al., 2012). This myokine was observed in both mice and humans, facilitating thermogenesis mechanism in adipose tissue, as promoting cortical bone genesis in bone (Colaianni et al., 2015; Erickson, 2013). Although the existence of irisin has been clearly defined by tandem mass spectrometry (MS) and enzyme-linked immunosorbent assays, its upstream signaling or adaptive characters in response to exercise stimulus has not been precisely defined (Jedrychowski et al., 2015; Kim et al., 2018). By far, data relative to irisin endocrine level of *in vivo* and its effective dose on regulating other tissues or organs are vigorous. *In vitro* researches prevalently adopted recombinant, rarely by conditional culture, but not endocrine irisin to investigate and quantified the dose effects (Colaianni et al., 2014; Kraemer et al., 2014; Qiao et al., 2016).

We herein first reported an exercise-mimicking model combined a myotubes and osteoblasts co-culture system with adjustable cyclic strain *in vitro* to question whether irisin is inducible in C2C12-derived myotubes, as well as irisin dose behaviors in response to variable mechanical force. Furthermore, this model was also developed to mimic the monodirectional endocrine signaling from muscle to skeleton to examine the bioactive function of irisin. Consequently, this model successfully induced cyclic strain-evoked bioactive irisin from C2C12 myotubes via activation of PGC-1α1 and PGC-1α4 signaling pathways, followed by encouraging the osteoblasts differentiation.

RESULTS

Cyclic mechanical force triggers a significant surge of irisin in C2C12-induced myotubes

When the confluence of C2C12 reaches 90%–100%, myoblasts start fusion and undergoes extremely limited proliferation in serum-deficient media, forming many fusion-competent myoblasts, which eventually develops to mature myotubes with multiple nuclei (Figure 1E) (Abmayr and Pavlath, 2012). Myotubes were observed after 2 days proliferation (Figure 1A) and 6 days differentiation (Figure 1B–1D) of C2C12 myoblasts. To characterize the phenotype of these myotubes, we first examined the expression of myofibrillar protein desmin and myoblast determination protein 1 (MyoD) family of transcription factors, i.e, Myogenin, MyoD, and Myogenic factor 5 (Myf5). All the determined markers expression in gene level were upregulated after 3 days differentiation except Desmin, which showed a robust increase at day 6, whereas no significant induction at day 3 compared to day 0 (Figure 1F). Western blots and quantification result also displayed significantly enhanced production of Myogenin and MyoD at day 6. Among all the transcriptional factors, only Myogenin expression both in gene and protein level gradually ascended with increasing differentiation time, consistent with the results reported that the muscle regulatory protein Myogenin accumulates in differentiated muscle cells when the culture medium is depleted for serum (Salminen et al., 1991).

To examine whether the mechanical force have effects on well differentiated myotubes, we developed a bioreactor by combining a cyclic strain system with a cell culture system. Myotubes attached on the silicone membranes were able to be deformed as the membrane was radially and cyclically stretched through vacuuming the air beneath, conducted by a controlling system (Figure 2A). To determine whether FNDC5 expressed in skeletal muscle cells is affected during the cyclic strain and whether different loading parameters have the ability to distinctively influence its expression, cells were exposed to strains with varying elongation including 5%, 8%, and 15% at 0.1Hz, 0.5Hz, and 1Hz. Given 3 h strain, FNDC5 expression with 5% expansion at all tested frequency, presented an obvious surge compared with static control group (0% elongation, 0Hz), as upregulation was comparable among different frequencies (Figure 2B-Left). Likewise, 15% elongation showed the same variation (Figure 2B-Middle). Unexpectedly, FNDC5 expression in 8% elongation, on the other hand, performed a fluctuating change following ascending frequency, as 0.5Hz dramatically increased FNDC5 expression contrast to 0.1 and 1 Hz (Figure 2B-Right).

Thus, we applied 0.5Hz to further examine how FNDC5 and irisin, encoded by FNDC5, response to different loading cycle, i.e, 1-day continuous cyclic stain versus 3 h intermittent cyclic stain per day within 8 days. In gene level, 24-h uninterrupted strain upregulated FNDC5 expression at both 12 h and 24 h, as

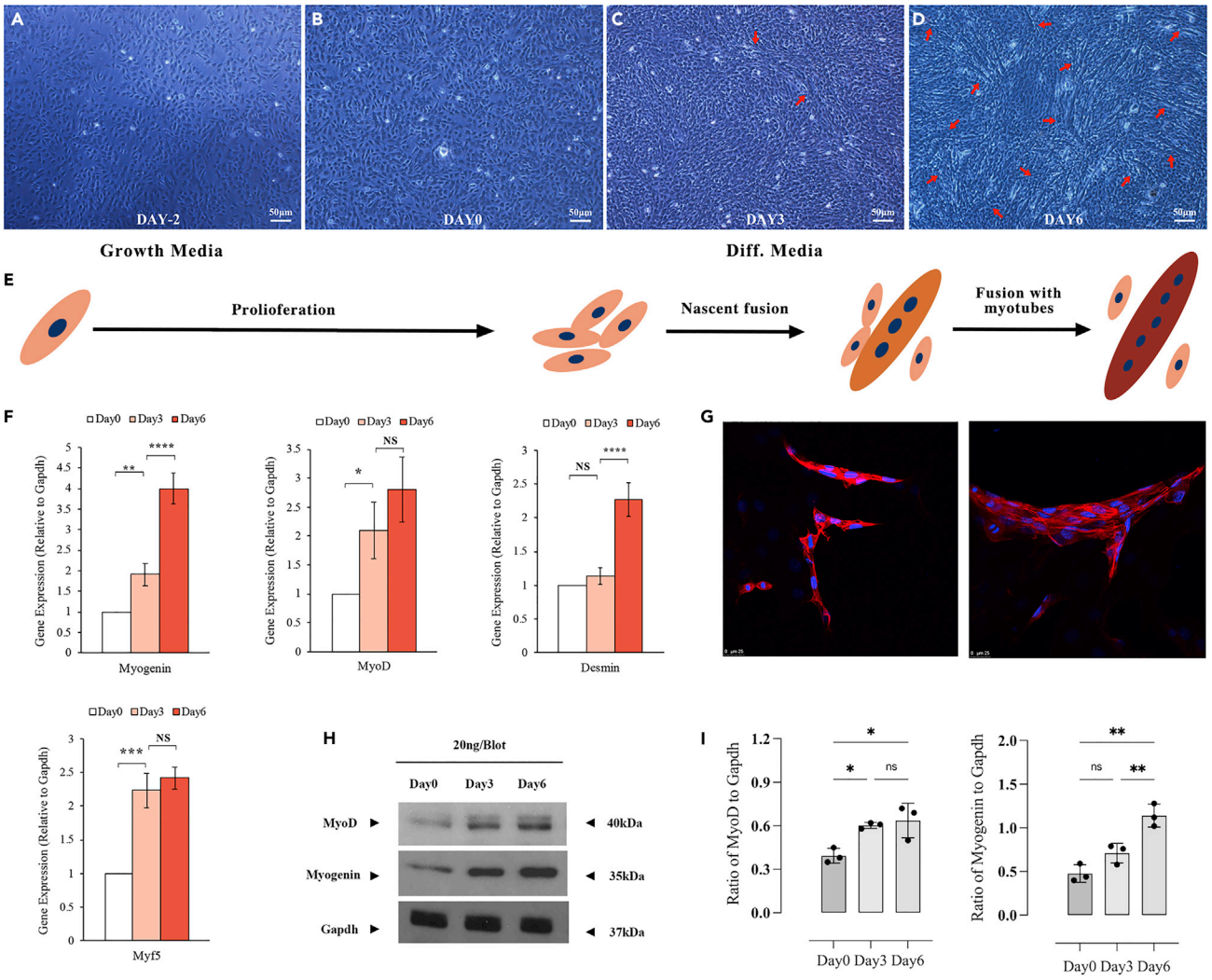

Figure 1. Characterization of contractile myotubes derived from C2C12

(A) C2C12 cells proliferation in growth media for 2 days.

(B) Differentiation progress at day 0, day 3(C), and day 6 (D) in the differentiation media. Scale bar: 50 μm.

(E) A schematic diagram represents the differentiation of myoblast cells toward mature myotubes.

(F) Key regulators expression during myogenesis at day 0, day 3, and day 6 by RT-PCR.

(G) Fluorescence pictures of nascent myoblasts fusion and myotubes. Scale bar: 25 μm.

(H) Protein expressions of regulators by Western blot.

(I) Quantification of blots. All protein concentrations were measured by BCA. Data are represented as mean ± SEM. Each scatterplots represents an independent biological experiment. Two-tailed *t*-test: p values: *p < 0.05, **p < 0.01, ***p < 0.001 and, ****p < 0.000.

24 h was apparently inferior to 12 h (Figure 2C-Left). Nevertheless, irisin was constantly secreted and accumulated, primarily 0.25 ± 0.15 ng/mL at 0 h followed by an increase to 1.69 ± 0.33 ng/mL at 12 h and 1.77 ± 0.59 ng/mL at 24 h, as no significant difference presented between 12 h and 24 h (Figure 2C-Right). Furthermore, cells apoptosis and death were observed after 1-day constant strain (Data not shown). This result indicated that inspite of descending FNDC5 expression with longer strain duration, irisin was continuously synthesized and accumulated in the media. However, FNDC5 upregulation at gene level was synchronized with irisin production (Figure 2D). FNDC5 gene expression was gradually enhanced from 0 days to 8 days (Figure 2D-Left); meanwhile, irisin concentration performed a time-dependent growth, initiated with 0.26 ± 0.1 ng/mL at 0 days and terminated with 1.89 ± 0.28 ng/mL at 8 days, in the presence of intermittent cyclic strain (Figure 2D-Right). Owing to the mild and lasting cyclic loading mode, cells are able to give rise to a constantly increasement, as a result, this approach was adopted to develop the further experiment exploring the irisin long-term behavior in response to mechanical force.

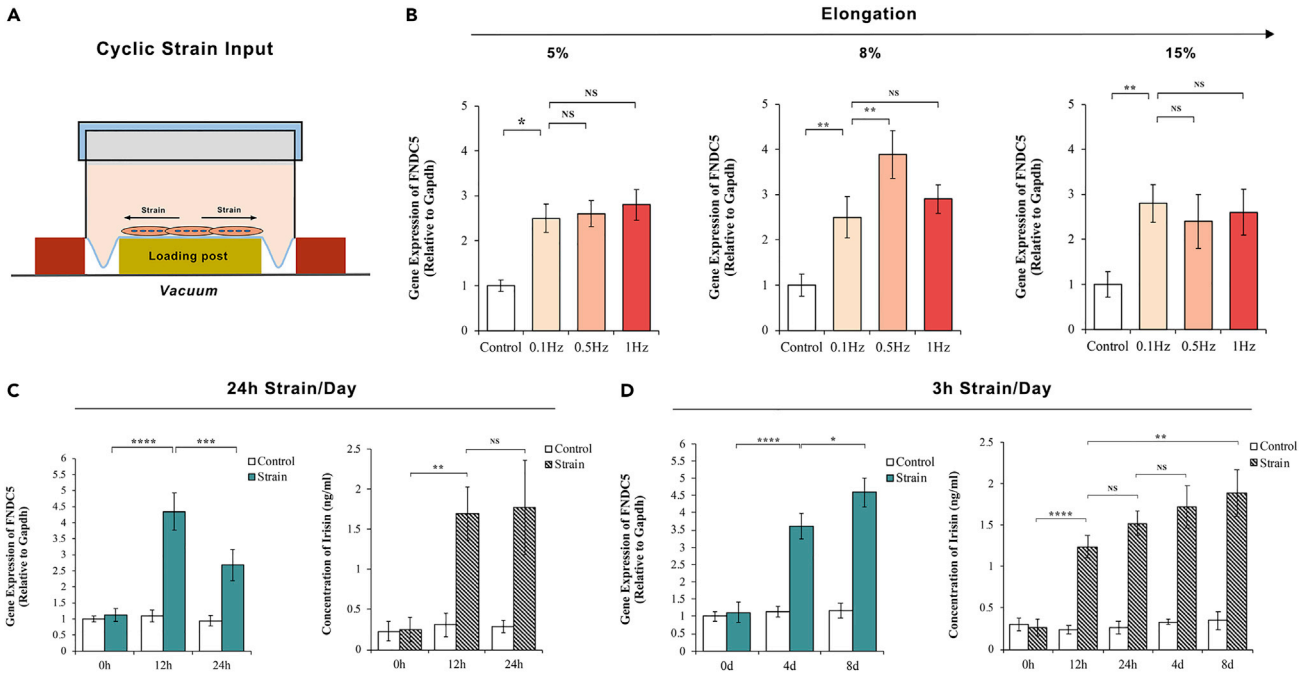

Figure 2. Irisin is inducible and increases in a time-dependent manner in myotubes contracted by cyclic strain

(A) Schematic representation of the adjustable cyclic strain loading system.

(B) Gene expression of FNDC5 with different cyclic strain parameters including 0.1, 0.5, and 1Hz frequency and 5%, 8%, and 15% elongation.

(C) Gene expression of FNDC5 and irisin production under 24 h continuous cyclic strain.

(D) Gene expression of FNDC5 and irisin production under intermittent cyclic stain (3 h per day within 8 days). Irisin concentrations were normalized by DNA concentrations. Data are represented as mean ± SEM Each scatterplots represents an independent biological experiment. One and two-way ANOVA test: p values: *p < 0.05, **p < 0.01, ***p < 0.001 and, ****p < 0.000.

These data indicate that cyclic strain triggered the FNDC5 gene and hence the release of irisin, although the possibility that irisin enhancement could also be ascribed to other mechanical force. Sensitive regulators are not able to be excluded.

FNDC5 knockout blocks irisin synthesis in C2C12-induced myotubes

To demonstrate the irisin production is linked with FNDC5 gene upregulation in response to cyclic strain, we successfully generated FNDC5KO C2C12 cell line and differentiated them into myotubes with myogenic markers well characterized (Figures S1 and 2). We first treated both WT cells and FNDC5 KO myotubes with the intermittent loading approach (3 h per day, 0.5Hz, 8% elongation) for 3 days. Culture media were immediately collected as the cyclic strain was halted (0 h after strain). Irisin concentration detected in the media, derived from WT C2C12 culture wells, was significantly elevated to 1.50 ± 0.28 ng/mL in strain group, by contrast to the control, which presented the baseline of irisin was quite low as 0.19 ± 0.06 ng/mL. Interestingly, less irisin level (0.33 ± 0.16 ng/mL) was detected from FNDC5 KO myotubes (Figure 3A), revealing that FNDC5 played an essential role on regulating the irisin generation under the mechanical force input. Curiously, irisin also exhibited a ceasing manner, successively decreased from 1.5 ± 0.28 ng/mL (0 h after strain) to 0.19 ± 0.11 ng/mL, over 2 h after pausing the strain (Figure 3A–3C).

To further evaluate the long-term effects of cyclic strain on irisin production, we also applied 2-week mild cyclic loading method to WT myotubes as well as FNDC5 myotubes. Notably, while the basic level of irisin concentration in control group at 14 days was comparable to the 3 days, irisin level in 14 days strain group was dramatically improved to 2.84 ± 0.32 ng/mL (0 days after strain), no longer elevated by 1 h after strain (1.42 ± 0.23 ng/mL), and, respectively, ceased to baseline by 2 h after strain (Figure 3D–3F). Especially, this improvement was blocked in FNDC5 KO group, convincing the effective impact of FNDC5 on irisin in response to the mechanical force.

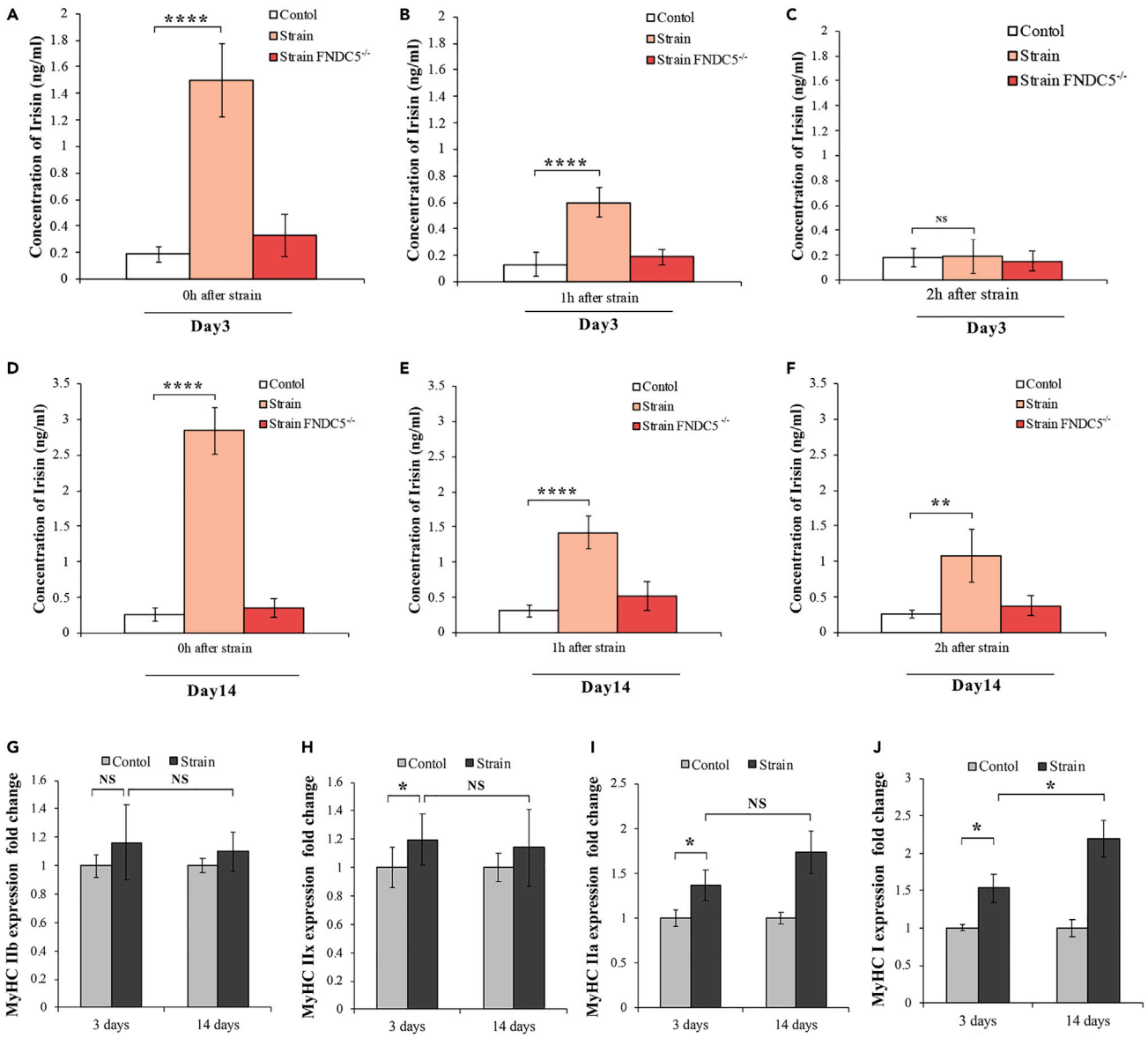

Figure 3. MHCs isoforms shift accounts for improved irisin levels with longer cyclic strain duration

(A–C) Irisin concentration in WT C2C12 myotubes and FNDC5 KO C2C12 myotubes at 0 h (A), 1 h (B), and 2 h (C) after suspending cyclic strain (0.5 Hz, 8% elongation, 3 h per day, 3 days).

(D–F) Irisin concentration in WT C2C12 myotubes and FNDC5 KO C2C12 myotubes at 0 h (D), 1 h (E), and 2 h (F) after suspending cyclic strain (0.5 Hz, 8% elongation, 3 h per day, 14 days).

(G–J) Different isoforms of the myosin heavy chains (MHCs) gene expression after 3 and 14 days intermittent cyclic strain. Irisin concentrations were normalized by DNA concentrations. Data are represented as mean ± SEM Each scatterplots represents an independent biological experiment. Two-tailed *t*-test and one-way ANOVA test: p values: *p < 0.05, **p < 0.01, ***p < 0.001 and, ****p < 0.000.

Given the irisin concentration adaptations to cyclic strain, myosin heavy chains (MyHC) were examined to explore the possibility that this adaptation is determined by the type of MyHC expressed throughout the tissue. MyHC is the motor protein of muscle thick filaments. There are four prevailing MHC genes, e.g, types I, IIa, IIx, and IIb, expressed in adult skeletal muscle cells, encoding proteins contribute to generating different fiber types including I, IIA, IIX, and IIB (Hyatt et al., 2016). Typically, these isoforms were classified by contractile speed, aerobic, or anaerobic characteristics, as fast fibers are usually identified as type II, comprising lower aerobic enzymes than slow fibers or type I fibers. Specifically, among the 4 fast isoforms, type IIa fibers have the most excellent oxidative capability followed by types IIx and types IIb, respectively.

In our case, we primally studied the gene expression of these 4 gene isoforms. Type IIa and I were more susceptible to mild cyclic strain, as their gene expression was maintained or increased further from 3 days to 14 days, indicating that mechanical stimulus applied in our study contributes to generate the type I fibers in myotubes (Figures 3G–3J).

To conclude, we demonstrated that FNDC5 plays a predominant role on irisin synthesis in contracted myotubes in our bioreactor. Furthermore, increased irisin secretory ability is ascribed to, at least in part, the shifts of MyHC isoforms from anaerobic type to aerobic type conducted by mechanical stimulus in myotubes.

PGC-1α1 and PGC-1α4 co-regulate irisin generation in contractile myotubes

PGC-1α, reported as a transcriptional coactivator, facilitates a fast to slow MyHC isoform transition when gene expression was elevated as a result of exercise, especially endurance exercise, rarely resistant exercise, in human skeletal muscle (Selsby et al., 2012). Overexpression of PGC-1α in skeletal muscle remarkably resists against muscle loss during aging (Ji and Kang, 2015). Four predominant isoforms of transcriptional products of PGC-1α gene were identified, termed PGC-1α1, PGC-1α2, PGC-1α3, and PGC-1α4. PGC-1α1 variant is responsible to inducing the oxidative capacity,;on the other hand, PGC-1α4 variant induces the muscle mass or hypertrophy phenotype (Ruas et al., 2012).

To investigate whether cyclic strain toward myotubes *in vitro* is comparable to the exercise toward skeletal muscle *in vivo*, we tested different transcripts expressed by PGC-1α gene. Clearly, owing to the cyclic strain (3 h per day), both PGC-1α1 and PGC-1α4 mRNA levels were enhanced by contrast to the PGC-1α2 and PGC-1α3 (Figure 4A). Additionally, testing that the translated protein levels of PGC-1α1 and PGC-1α4 synchronized with mRNA expression, we confirmed the PGC-1α1 and PGC-1α4 were more susceptible to mechanical force loaded in our system (Figures 4B and 4C). Based on our results that higher irisin production is associated with the MyHC isoforms shift prone to aerobic type, as well as the similar role of PGC-1α4 variant, we inhibited the PGC-1α1 and PGC-1α4 mRNA expression by RNAi. Two distinct siRNA were designed, termed siPGC-1α1 and siPGC-1α4. Owing to an overlapped region existed on both mRNA transcripts, the PGC-1α1 transcript, the longer one, carries an additional region than PGC-1α4. Thus, siPGC-1α1s was designed to specifically target on its additional arm. Consequently, siPGC-1α4 was able to non-specifically interfere the PGC-1α4 mRNA, what's more, equivalent regions on PGC-1α1 mRNA (Figure 4D). Dramatical reduction of PGC-1α1 and PGC-1α4 mRNAs was observed in strain groups with solely addition of siPGC-1α1, siPGC-1α4, or both (Figures 4E and 4F), as siPGC-1α4 was exactly able to reduce both mRNAs. We also probed the corresponding irisin concentrations in each group. siRNAs compromised the irisin enhancement elevated by cyclic strain. Addition of siPGC-1α1 mildly brought the irisin concentration from 1.6 $\pm$ 0.28 ng/mL down to 0.94 $\pm$ 0.14 ng/mL. Further decline (0.18 $\pm$ 0.07 ng/mL) was found in combined siPGC-1α1 and siPGC-1α4 group (Figure 4G). In addition, blot result also showed that RNA interfering gave rise to the decline of PGC-1α1 and PGC-1α4 mRNAs, whereas cyclic strain could augment them (Figures 4H and 4I).

Taken together, cyclic mechanical strain we conducted by the bioreactor induced the PGC-1α1 and PGC-1α4 mRNAs expression, rather than PGC-1α2 and PGC-1α3, contributed to the generation of irisin in myotubes *in vitro*.

Contraction-induced irisin from C2C12 myotubes promotes osteogenesis in MC3T3 cells

To examine whether the released irisin is bioactive, we conducted another experiment to co-culture contractile C2C12 myotubes and MC3T3 osteoblasts in the bioreactor, which was designed to mimicking the endocrine pathways in skeletal muscle system *in vivo* (Figure 5A). Osteoblasts seeded on the transwells with bores allowing small molecular to transmit through were conditional co-cultured with WT and FNDC5 KO C2C12 myotubes. Irisin released from contracted myotubes was able to be detected. Here, we hypothesized that secreted irisin functioned on the osteoblasts. Serum irisin concentrations are positively associated with bone quality, as irisin is a strong determinant of bone remodeling and new bone formation, especially cortical bone mass, in mice studies (Colaianni et al., 2015).

To explore whether induced irisin is able to functionally affect osteoblasts differentiation, we determined to characterize it using osteogenic transcription factors, e.g, Runx2, Osx, Atf4, Spp1, and Sost, as wells as differentiation makers including Alp, Cola1, and Ocn. Runx2 was activated at the earlier stage and

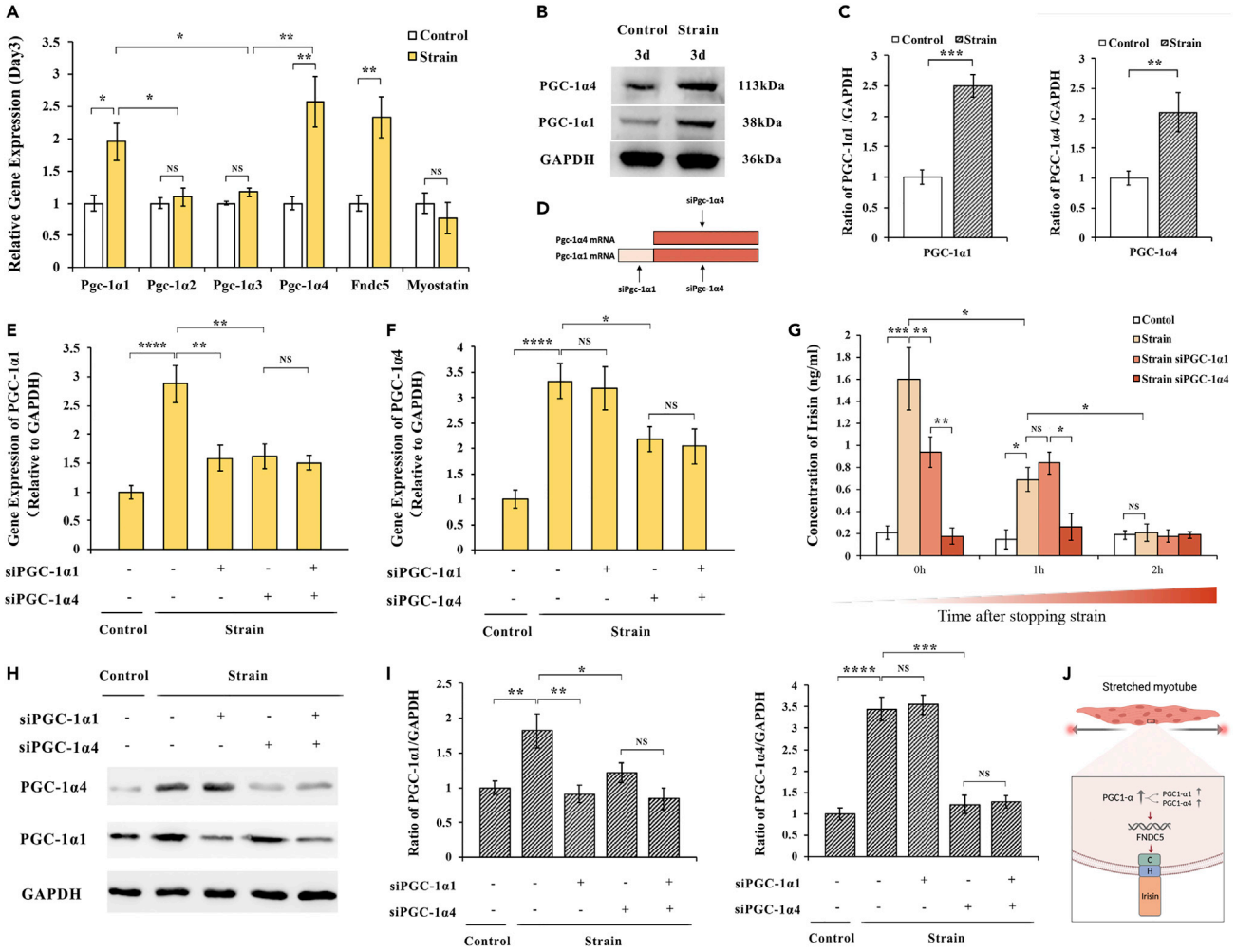

Figure 4. PGC-1α1 and PGC-1α4 are both increased in contractile C2C12 myotubes

(A) Different isoforms of PGC-1α, FNDC5, and Myostatin gene expression after 3 days cyclic strain (3 h per day).

(B–C) Protein expressions of PGC-1α1, PGC-1α4, and GAPDH by Western blot (B) and (C) quantification results.

(D) Diagram schematizing siRNA targeting sites on PGC-1α1and PGC-1α4 mRNA.

(E–F) RNA interfering on PGC-1α1(E) and PGC-1α4 (F) gene expression (G) RNA interfering on irisin production in C2C12 myotubes.

(H–J) RNA interfering on PGC-1α1 and PGC-1α4 protein expression (H) and quantification results (I). (J) Schematic diagram showing irisin synthesis is regulated by PGC-1α isoforms. All protein concentrations were measured by BCA. Irisin concentrations were normalized by DNA concentrations. Data are represented as mean ± SEM Each scatterplots represents an independent biological experiment. Two-tailed *t*-test, one and two-way ANOVA test: p values: *p < 0.05, **p < 0.01, ***p < 0.001 and, ****p < 0.000.

responsible to induce the preosteoclasts into mature osteoblasts, as well as arousing the expression of downstream osteoblast-related genes. In our study, after 3 days of cyclic strain on myotubes, Runx2 was significantly increased in WT myotubes conditionally cultured niche, compared with control group, and subsequently enhanced after another 11 days of strain (Figure 5B). Significantly, lower Runx2 expression was found in the MC3T3 cells co-cultured with FNDC5 KO myotubes, indicating that the genetic loss deprived the irisin generation. Meanwhile, the downstream transcriptional factor including Atf4 and Spp1 and markers including Alp and Cola1 was also increased; however, in an opposite way, Sost, a negative transcriptional factor on osteogenesis, was downregulated by the strain (Figures 5C, 5D, 5F, and 5G). Besides, we also cultured MC3T3 cells without any types of myotubes to eliminate the possibility of self-induced difference from C2C12 myotubes. Under the strain, there was no significant difference between FNDC5 KO myotubes co-culture group and MC3T3 group, demonstrating that upon regulation on osteoblast differentiation, blocking the FNDC5 gene in myotubes was equivalent to absence of myotubes.

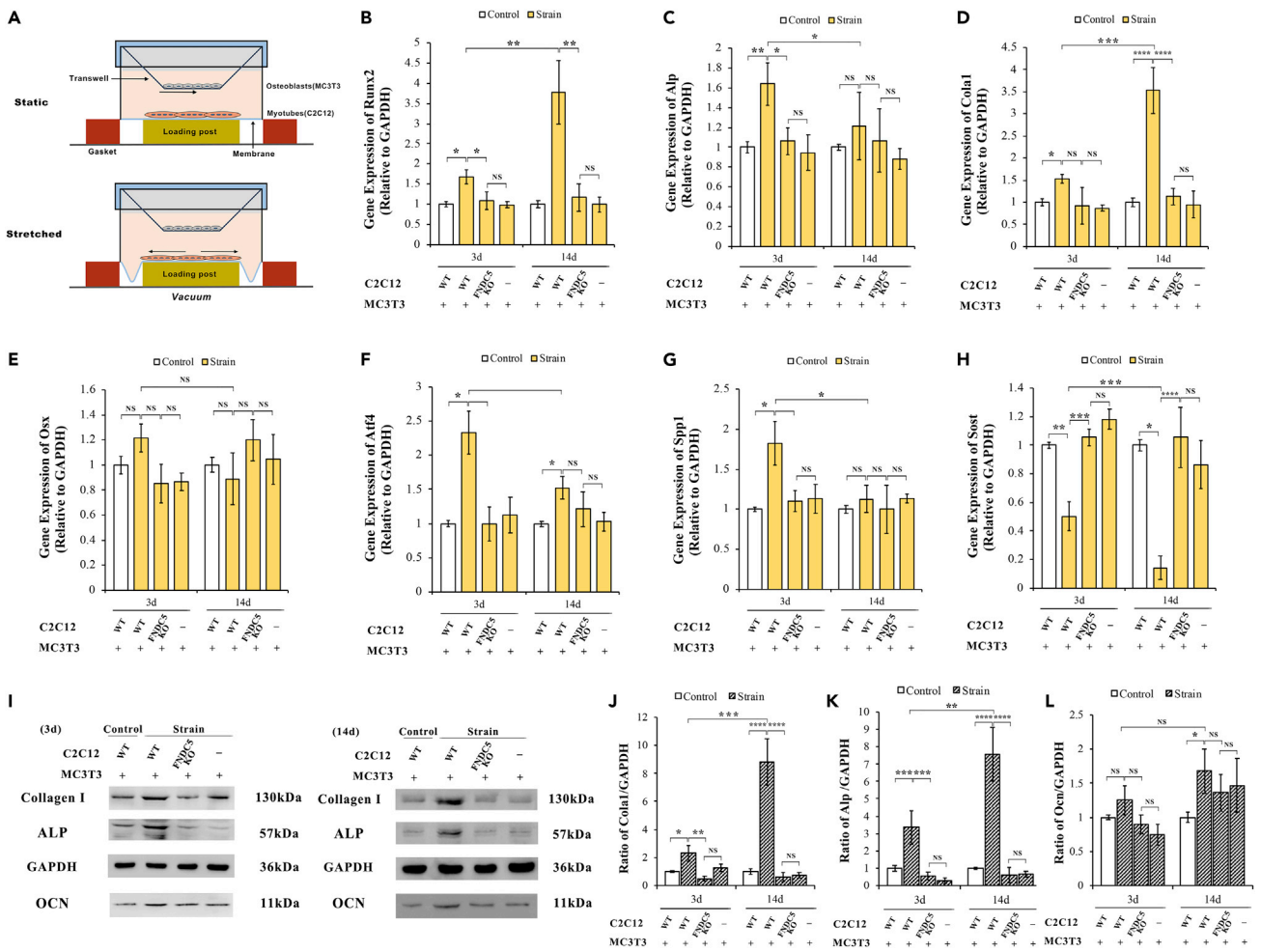

Figure 5. Contraction-induced irisin from C2C12 myotubes promotes MC3T3 cells differentiation

(A) Schematic diagram of the co-culture system and mechanical force loading.

(B–H) Osteogenesis regulatory markers gene expression in conditionally cultured MC3T3 cells after 3 and 14 days strain (3 h per day). (I–L) Blots results (I) and quantification results of osteogenesis regulatory markers protein expression in conditionally cultured MC3T3 cells after 3 and 14 days strain (3 h per day). All protein concentrations were measured by BCA. Data are represented as mean ± SEM Each scatterplots represents an independent biological experiment. Two-tailed *t*-test, one and two-way ANOVA test: p values: *p < 0.05, **p < 0.01, ***p < 0.001 and, ****p < 0.000.

In the post-differentiation stage (14 days), with the irisin induce by cyclic strain accumulated to a higher level, Runx2 and Cola1 mRNAs enriched even further than 3 days in WT myotubes, whereas this enrichment was not observed in FNDC5 KO myotubes. Western blots also presented the correspondingly similar results, as cola1 continue accumulating in MC3T3 cells throughout the whole differentiation phase (Figures 5I and 5J). Particularly, another typical osteogenic differentiation protein detected was also significantly increased in the WT myotubes strain group, while in the FNDC5 KO myotubes was not at day 14 (Figure 5L).

In all, data derived from our experiment showed that contraction-induced irisin from C2C12 myotubes promoted osteogenesis in MC3T3 cells, while this regulation was able to be dismissed as the FNDC5 was absent.

DISCUSSION

Substantial progress occurs inside skeletal muscle during physical exercise, subsequently releasing irisin positively influence proximal and distill tissues through blood circulation (Boström et al., 2012; Colaianni et al., 2014, 2015, 2019; Jedrychowski et al., 2015; Kim et al., 2018; Qiao et al., 2016). ATP depletion, a state

of metabolic demand in response to contraction of skeletal muscle, can evoke a significant surge of irisin concentration, which is able to maintain ATP homeostasis during exercise (Huh et al., 2012, 2014; Perakakis et al., 2017). Skeletal muscle has been demonstrated to be engineered *in vitro* by culturing and differentiating C2C12 myoblasts into nascent or mature myotubes (Lautaoja et al., 2020). Mechanical stretch triggers mechanical-sensitive pathways initially through transmembrane integrin on muscle and subsequently transcriptional response to promote muscle anabolic signaling and generation (Chambers et al., 2009; De Deyne, 2001; Gao and Carson, 2016; Zöllner et al., 2012). In addition to muscle growth, myokine release has also been observed in passively stretched C2C12 myotubes (Zöllner et al., 2012). In common to these researches, we conducted the cyclic strain to symmetrically stretching the C2C12 cells via synchronously stretching the cells seeded silicone membrane (Figure 2A). However, differently, we first induced the myotubes statically *in vitro*, followed by co-culturing with osteoblasts to intimate the endocrine signaling in musculoskeletal unit (Figure 5A). Cells reached to 90% confluence after 2 days proliferation, followed by 6 days serum-deficient media culturing; as a result, myoblasts fusion formed, as multi-directional arrays of myotubes were observed which are 2–4 times longer than myotubes grown under static culture conditions. Myogenic transcriptional factors and proteins were significantly enhanced in myotubes during maturing phase, indicating the phenotypes of myotubes were successfully characterized (Figures 1F, 1H, and 1I).

Based on previous studies, we investigated different portfolios of parameters including 5%, 8%, and 15% in elongation and 0.1Hz, 0.5Hz, and 1Hz in frequency (Chang et al., 2016; Gao and Carson, 2016; Jin et al., 2019; Turner et al., 2008). Afterwards, a moderate stretching intensity was adopted in lines with our results that myotubes contracted at 0.5Hz with 10% elongation performed the most optimized FNDC5 expression. In human studies, moderate aerobic exercise is a form of exercise widely used on plasma irisin responses (Boström et al., 2012; Huh et al., 2012). Aerobic training was reported that it could induce a greater irisin concentration (4.3 ng/mL) than sedentary (3.6 ng/mL) in humans (Jedrychowski et al., 2015). Daily aerobic exercise time differs in a series of human and animal study. Data from a human study showed that one-time 40 min of aerobic running was able to increase serum irisin level (Ozbay et al., 2020), while serum irisin was significantly higher in both sedentary hyper- and hypothyroid rats after 100-min forced swimming (Samy et al., 2015). Distinguishing from somatic movement, our skeletal muscle model adopted a longer non-continuous loading mode (3 h per day). Intriguingly, 8 days of cyclic strain eventually elevated the irisin level from 0.26 $\pm$ 0.1 ng/mL to 1.89 $\pm$ 0.28 ng/mL (Figure 2D). Furthermore, consistent with one of our experimental hypotheses, FNDC5 knockout blocks irisin synthesis in myotubes, exposing that irisin was inducible in our system, as well as offering the possibilities to further explore the mechanism of irisin react to mechanical stimulus.

Our data also revealed a time-dependent manner of irisin concentrations. Long-term cyclic strain (14days) had a greater stimulation on irisin generation than short-term cyclic strain (3days), as MyHC isoforms expression in contracted myotubes indicated a shift tendency from anaerobic to aerobic types adapting to the long-term moderate stretching. *In vitro*, similar shift from faster MyHCIIb to IIa and even I has been previously observed (Kurokawa et al., 2007). Increased myotube size measured by diameter is chronical stretch and MyHC expression relevant (Gao and Carson, 2016). *In vivo*, consistent adaptive phenotype alterations from faster to slower MyHC isoforms have been demonstrated as results of endurance and resistance exercise (Colaianni et al., 2017; Staron et al., 1994). However, the transduction signaling associated with this phenotype switch needs to be further unveiled. Moreover, irisin was dramatically improved by 0 days after strain (2.84 $\pm$ 0.32 ng/mL), no longer elevated by 1 h after strain (1.42 $\pm$ 0.23 ng/mL), and, respectively, ceased to baseline by 2 h after strain. In other words, irisin induced by cyclic strain gradually ceased to a baseline level over 2 h. The evidence supported our conclusion from another study resented that an increase in concentrations of irisin response to 54 min treadmill subsequently declined by 90 min of steady-state exercise in groups of young men and women (Kraemer et al., 2014). Although the irisin concentrations *in vivo* and *in vitro* are not comparable, the conclusions on proving a rapid cessation of irisin in the absence of exercise/mechanical stimulus are consistent.

If the muscle is described to primary metabolic communicator to transmit external mechanical stimulus toward physiological signaling, PGC-1α then is the ''rheostat'' to export and control the mechanical force or contractile activities (Islam et al., 2018). Under a specific external stimulation, such as physical exercise, PGC-1α can be transformed into 4 primary isoforms signaling at different downstream regulatory pathways,

eventually adapting the specific stimulation on structure and function (Chinsomboon et al., 2009). Our findings are relevant to exposing the possible upstream signaling of irisin and defining that PGC-1α1 and PGC-1α4 mRNAs expression, but not PGC-1α2 and PGC-1α3, contributed to the generation of irisin in myotubes *in vitro*, as PGC-1α1 and PGC-1α4 were more susceptible to mechanical force loaded in our system.

Another significant purpose of our study was trying to establish a skeletal muscle endocrine/paracrine system to further identify the biofunction of induced irisin as a secreted protein or hormone. In agreement with our hypothesis on the bioactive function of myotubes-secreted irisin, it is able to positively affect the differentiation of osteoblasts on both primary phase and terminal phase (Figure 5B–5L). Intriguingly, similar preciously published data reported that single direction dynamic stretch loaded on the substratum, on which myoblasts were seeded for 3 days at a rate of 0.35 mm/h, was adopted to simulate *in vivo* bone elongation during development (Vandenburgh and Karlisch, 1989). Induced irisin was prone to activate osteogenic transcription factors, e.g, Runx2, Osx, Atf4, Spp1, and Sost, as wells as differentiation makers including Alp, Cola1, and Ocn (Franceschi et al., 2007; Komori, 2006). The observation that no significant difference between static group and FNDC5 KO group for each osteogenic marker, suggests that FNDC5 plays a predominant role on irisin synthesis, and the genetic loss of FNDC5 may compromise the irisin releasing that should have been induced by cyclic strain, and ultimately barely affected the conditionally cultured osteoblasts.

The musculoskeletal unit we developed allows us to produce secreted mediator-irisin in engineered contractile skeletal muscle and evaluate the adaptive irisin concentrations range using various different parameter combinations *in vitro*. The applied mechanical stimulus promotes irisin generation via upregulating PGC-1α1 and PGC-1α4 expression, and successfully analogs the exercise-induced bioactive irisin, which confers positive influence on osteoblasts differentiation. Though we do not know how biologically precisely does this musculoskeletal unit mimics physiological muscle skeleton interacting system, it is of interest to note its potential to conveniently identify adaptive changes in mechanically stimulated muscle and metabolism in response to outer exercise-mimetic stimulus, and crosstalk with other tissue types. Moreover, with this model we will further take the advantage of ongoing technical innovations, for example the SC RNA-seq, to improve our understanding of skeletal muscle signaling pathways associated with mechanical stimulation, and profiling their molecular mechanisms.

Limitations of the study

One goal of this study is primarily to illuminate whether and how irisin is response to the mechanical force in exercising skeletal muscle *in vitro*. Ideally, the primary skeletal muscle tissue, including components like myofibers, connective tissue, and adipose tissue, is supposed to be applied in this model. However, it is challenging to perform the isolated primary muscle tissue in this culturing system while maintaining its physiological traits. Alternatively, we differentiated C2C12 cells from myoblasts to the myotube-like tissue and well-characterized the phenotype of these myotubes by examining the expression of myofibrillar protein such as Desmin, Myogenin, and MyoD in both transcriptional level and translational level. Ability to improve the engineered muscle, structurally and functionally restore it to primary muscle unit would further strengthen our model.

Although any steps of myogenesis can be recapitulated through *in vitro* differentiation of immortalized myogenic cells C2C12 into myotubes, which has been well established in previous studies as well as our study, we were carefully considering primary myoblasts as our experimental subject during our experiment design stage. Given that they have been suggested as the most physiologically relevant model for studying myogenesis *in vitro*, however, due to their low abundance in adult skeletal muscle, isolation of primary myoblasts is technically challenging.

STAR★METHODS

Detailed methods are provided in the online version of this paper and include the following:

- KEY RESOURCES TABLE
- RESOURCE AVAILABILITY
  - Lead contact
  - Materials availability

SUPPLEMENTAL INFORMATION

Supplemental information can be found online at https://doi.org/10.1016/j.isci.2022.104135.

ACKNOWLEDGMENTS

The study was supported by National Natural Science Foundation of China (No. 11822201, 11827803, U20A20390). We gratefully acknowledge NSFC and all our collaborators.

AUTHOR CONTRIBUTIONS

L.W. and H.K. conceived experiments, C.L. and Y.F. conducted experiments, and Y.Z. carried out experiments and analyzed the results. Y.Z. wrote the manuscript. All authors reviewed and revised the manuscript.

DECLARATION OF INTERESTS

The authors declare no competing interests.

Received: January 1, 2022
Revised: February 28, 2022
Accepted: March 17, 2022
Published: April 15, 2022

REFERENCES

Aas, V., Bakke, S.S., Feng, Y.Z., Kase, E.T., Jensen, J., Bajpeyi, S., Thoresen, G.H., and Rustan, A.C. (2013). Are cultured human myotubes far from home? Cell Tissue Res. *354*, 671–682. https://doi.org/10.1007/S00441-013-1655-1/FIGURES/4.

Abmayr, S.M., and Pavlath, G.K. (2012). Myoblast fusion: lessons from flies and mice. Development *139*, 641–656. https://doi.org/10.1242/DEV.068353.

Aguilar-Agon, K.W., Capel, A.J., Martin, N.R.W., Player, D.J., and Lewis, M.P. (2019). Mechanical loading stimulates hypertrophy in tissue-engineered skeletal muscle: molecular and phenotypic responses. J. Cell. Physiol. *234*, 23547. https://doi.org/10.1002/JCP.28923.

Baar, K. (2006). Training for endurance and strength: lessons from cell signaling. Med. Sci. Sports Exerc. *38*, 1939–1944. https://doi.org/10.1249/01.MSS.0000233799.62153.19.

Bodine, S.C., Stitt, T.N., Gonzalez, M., Kline, W.O., Stover, G.L., Bauerlein, R., Zlotchenko, E., Scrimgeour, A., Lawrence, J.C., Glass, D.J., and Yancopoulos, G.D. (2001). Akt/mTOR pathway is a crucial regulator of skeletal muscle hypertrophy and can prevent muscle atrophy in vivo. Nat. Cell Biol. *311*, 1014–1019. https://doi.org/10.1038/ncb1101-1014.

Booth, F.W., Roberts, C.K., and Laye, M.J. (2012). Lack of exercise is a major cause of chronic diseases. Compr. Physiol. *2*, 1143. https://doi.org/10.1002/CPHY.C110025.

Boström, P., Wu, J., Jedrychowski, M.P., Korde, A., Ye, L., Lo, J.C., Rasbach, K.A., Boström, E.A., Choi, J.H., Long, J.Z., et al. (2012). A PGC1-α-dependent myokine that drives brown-fat-like development of white fat and thermogenesis. Nature *481*, 463–468. https://doi.org/10.1038/NATURE10777.

Cartee, G.D., Hepple, R.T., Bamman, M.M., and Zierath, J.R. (2016). Exercise promotes healthy aging of skeletal muscle. Cell Metab *23*, 1034–1047. https://doi.org/10.1016/j.cmet.2016.05.007.

Chambers, M.A., Moylan, J.S., Smith, J.D., Goodyear, L.J., and Reid, M.B. (2009). Stretch-stimulated glucose uptake in skeletal muscle is mediated by reactive oxygen species and p38 MAP-kinase. J. Physiol. *587*, 3363–3373. https://doi.org/10.1113/JPHYSIOL.2008.165639.

Chang, Y.J., Chen, Y.J., Huang, C.W., Fan, S.C., Huang, B.M., Chang, W.T., Tsai, Y.S., Su, F.C., and Wu, C.C. (2016). Cyclic stretch facilitates myogenesis in C2C12 myoblasts and rescues thiazolidinedione-inhibited myotube formation. Front. Bioeng. Biotechnol. *4*. https://doi.org/10.3389/FBIOE.2016.00027.

Chinsomboon, J., Ruas, J., Gupta, R.K., Thom, R., Shoag, J., Rowe, G.C., Sawada, N., Raghuram, S., and Arany, Z. (2009). The transcriptional coactivator PGC-1α mediates exercise-induced angiogenesis in skeletal muscle. Proc. Natl. Acad. Sci. U S A *106*, 21401–21406. https://doi.org/10.1073/pnas.0909131106.

Clevers, H. (2016). Modeling development and disease with organoids. Cell *165*, 1586–1597. https://doi.org/10.1016/J.CELL.2016.05.082.

Colaianni, G., Cuscito, C., Mongelli, T., Oranger, A., Mori, G., Brunetti, G., Colucci, S., Cinti, S., and Grano, M. (2014). Irisin enhances osteoblast differentiation in vitro. Int. J. Endocrinol. *2014*. https://doi.org/10.1155/2014/902186.

Colaianni, G., Cuscito, C., Mongelli, T., Pignataro, P., Buccoliero, C., Liu, P., Lu, P., Sartini, L., Comite, M.D., Mori, G., et al. (2015). The myokine irisin increases cortical bone mass. Proc. Natl. Acad. Sci. U S A *112*, 12157–12162. https://doi.org/10.1073/PNAS.1516622112.

Colaianni, G., Mongelli, T., Cuscito, C., Pignataro, P., Lippo, L., Spiro, G., Notarnicola, A., Severi, I., Passeri, G., Mori, G., et al. (2017). Irisin prevents and restores bone loss and muscle atrophy in hind-limb suspended mice. Sci. Rep. *71*, 1–16. https://doi.org/10.1038/s41598-017-02557-8.

Colaianni, G., Sanesi, L., Storlino, G., Brunetti, G., Colucci, S., and Grano, M. (2019). Irisin and bone: from preclinical studies to the evaluation of its circulating levels in different populations of human subjects. Cells *8*, 451. https://doi.org/10.3390/CELLS8050451.

Collinsworth, A.M., Torgan, C.E., Nagda, S.N., Rajalingam, R.J., Kraus, W.E., and Truskey, G.A. (2000). Orientation and length of mammalian skeletal myocytes in response to a unidirectional stretch. Cell Tissue Res *302*, 243–251. https://doi.org/10.1007/S004410000224.

De Deyne, P.G. (2001). Application of passive stretch and its implications for muscle fibers. Phys. Ther. *81*, 819–827. https://doi.org/10.1093/PTJ/81.2.819.

Erickson, H.P. (2013). Irisin and FNDC5 in retrospect: an exercise hormone or a transmembrane receptor? Adipocyte *2*, 289–293. https://doi.org/10.4161/ADIP.26082.

Franceschi, R.T., Ge, C., Xiao, G., Roca, H., and Jiang, D. (2007). Transcriptional regulation of osteoblasts. Ann. N. Y. Acad. Sci. *1116*, 196–207. https://doi.org/10.1196/ANNALS.1402.081.

Gao, S., and Carson, J.A. (2016). Lewis lung carcinoma regulation of mechanical stretch-induced protein synthesis in cultured myotubes. Am. J. Physiol. Cell Physiol. *310*, C66–C79. https://doi.org/10.1152/AJPCELL.00052.2015.

Hawley, J.A., Hargreaves, M., Joyner, M.J., and Zierath, J.R. (2014). Integrative biology of exercise. Cell *159*, 738–749. https://doi.org/10.1016/J.CELL.2014.10.029.

Hoppeler, H., Baum, O., Lurman, G., and Mueller, M. (2011). Molecular mechanisms of muscle plasticity with exercise. Compr. Physiol. *1*, 1383–1412. https://doi.org/10.1002/CPHY.C100042.

Huh, J.Y., Mougios, V., Kabasakalis, A., Fatouros, I., Siopi, A., Douroudos, I.I., Filippaios, A., Panagiotou, G., Park, K.H., and Mantzoros, C.S. (2014). Exercise-induced irisin secretion is independent of age or fitness level and increased irisin may directly modulate muscle metabolism through AMPK activation. J. Clin. Endocrinol. Metab. *99*, E2154–E2161. https://doi.org/10.1210/JC.2014-1437.

Huh, J.Y., Panagiotou, G., Mougios, V., Brinkoetter, M., Vamvini, M.T., Schneider, B.E., and Mantzoros, C.S. (2012). FNDC5 and irisin in humans: I. Predictors of circulating concentrations in serum and plasma and II. mRNA expression and circulating concentrations in response to weight loss and exercise. Metabolism *61*, 1725–1738. https://doi.org/10.1016/J.METABOL.2012.09.002.

Hyatt, J.P.K., Nguyen, L., Hall, A.E., Huber, A.M., Kocan, J.C., Mattison, J.A., de Cabo, R., LaRocque, J.R., and Talmadge, R.J. (2016). Muscle-specific myosin heavy chain shifts in response to a long-term high fat/high sugar diet and resveratrol treatment in nonhuman primates. Front. Physiol. *7*. https://doi.org/10.3389/FPHYS.2016.00077.

Islam, H., Edgett, B.A., and Gurd, B.J. (2018). Coordination of mitochondrial biogenesis by PGC-1α in human skeletal muscle: a re-evaluation. Metabolism *79*, 42–51. https://doi.org/10.1016/J.METABOL.2017.11.001.

Jedrychowski, M.P., Wrann, C.D., Paulo, J.A., Gerber, K.K., Szpyt, J., Robinson, M.M., Nair, K.S., Gygi, S.P., and Spiegelman, B.M. (2015). Detection and quantitation of circulating human irisin by tandem mass spectrometry. Cell Metab. *22*, 734–740. https://doi.org/10.1016/J.CMET.2015.08.001.

Ji, L.L., and Kang, C. (2015). Role of PGC-1α in sarcopenia: etiology and potential intervention - a mini-review. Gerontology *61*, 139–148. https://doi.org/10.1159/000365947.

Jin, J., Stevenson Moylan, J., Hughes, D.C., Xue, Z., Baccam, A., Benoni-Sviercovich, A., Rocchi, M., Moresi, V., Seelaender, M., Li, Z., et al. (2019). The Mechanical Stimulation of Myotubes Counteracts the Effects of Tumor-Derived Factors Through the Modulation of the Activin/Follistatin Ratio. Front Physiol. https://doi.org/10.3389/fphys.2019.00401.

Juffer, P., Jaspers, R.T., Klein-Nulend, J., and Bakker, A.D. (2014). Mechanically loaded myotubes affect osteoclast formation. Calcif. Tissue Int. *94*, 319–326. https://doi.org/10.1007/S00223-013-9813-8.

Kim, H., Wrann, C.D., Jedrychowski, M., Vidoni, S., Kitase, Y., Nagano, K., Zhou, C., Chou, J., Parkman, V.J.A., Novick, S.J., et al. (2018). Irisin mediates effects on bone and fat via αV integrin receptors. Cell *175*, 1756–1768.e17. https://doi.org/10.1016/J.CELL.2018.10.025.

Komori, T. (2006). Regulation of osteoblast differentiation by transcription factors. J. Cell. Biochem. *99*, 1233–1239. https://doi.org/10.1002/JCB.20958.

Kraemer, R.R., Shockett, P., Webb, N.D., Shah, U., and Castracane, V.D. (2014). A transient elevated irisin blood concentration in response to prolonged, moderate aerobic exercise in young men and women. Horm. Metab. Res. *46*, 150–154. https://doi.org/10.1055/S-0033-1355381.

Kurokawa, K., Abe, S., Sakiyama, K., Takeda, T., Ide, Y., and Ishigami, K. (2007). Effects of stretching stimulation with different rates on the expression of MyHC mRNA in mouse cultured myoblasts. Biomed. Res. *28*, 25–31. https://doi.org/10.2220/BIOMEDRES.28.25.

Lautaoja, J.H., Pekkala, S., Pasternack, A., Laitinen, M., Ritvos, O., and Hulmi, J.J. (2020). Differentiation of murine C2C12 myoblasts strongly reduces the effects of Myostatin on intracellular signaling. Biomolecules *10*, 695. https://doi.org/10.3390/BIOM10050695.

Mahoney, D.J., Parise, G., Melov, S., Safdar, A., and Tarnopolsky, M.A. (2005). Analysis of global mRNA expression in human skeletal muscle during recovery from endurance exercise. FASEB J. *19*, 1498–1500. https://doi.org/10.1096/FJ.04-3149FJE.

Massart, J., Sjögren, R.J.O., Egan, B., Garde, C., Lindgren, M., Gu, W., Ferreira, D.M.S., Katayama, M., Ruas, J.L., Barrès, R., et al. (2021). Endurance exercise training-responsive miR-19b-3p improves skeletal muscle glucose metabolism. Nat. Commun. *121 12*, 1–13. https://doi.org/10.1038/s41467-021-26095-0.

Moustogiannis, A., Philippou, A., Zevolis, E., Taso, O., Chatzigeorgiou, A., and Koutsilieris, M. (2020). Characterization of optimal strain, frequency and duration of mechanical loading on skeletal myotubes' biological responses. In Vivo *34*, 1779–1788. https://doi.org/10.21873/INVIVO.11972.

Ozbay, S., Ulupinar, S., Şebin, E., and Altinkaynak, K. (2020). Acute and chronic effects of aerobic exercise on serum irisin, adropin, and cholesterol levels in the winter season: indoor training versus outdoor training. Chin. J. Physiol. *63*, 21–26. https://doi.org/10.4103/CJP.CJP_84_19.

Pedersen, B.K., and Febbraio, M.A. (2012). Muscles, exercise and obesity: skeletal muscle as a secretory organ. Nat. Rev. Endocrinol. *8*, 457–465. https://doi.org/10.1038/NRENDO.2012.49.

Perakakis, N., Triantafyllou, G.A., Manuel Fernández-Real, J., Huh, J.Y., Park, K.H., Seufert, J., and Mantzoros, C.S. (2017). Physiology and role of irisin in glucose homeostasis HHS Public Access. Nat. Rev. Endocrinol. *13*, 324–337. https://doi.org/10.1038/nrendo.2016.221.

Pillon, N.J., Gabriel, B.M., Dollet, L., Smith, J.A.B., Sardón Puig, L., Botella, J., Bishop, D.J., Krook, A., and Zierath, J.R. (2020). Transcriptomic profiling of skeletal muscle adaptations to exercise and inactivity. Nat. Commun. *11*, 1–15. https://doi.org/10.1038/S41467-019-13869-W.

Qiao, X.Y., Nie, Y., Ma, Y.X., Chen, Y., Cheng, R., Yinrg, W.Y., Hu, Y., Xu, W.M., and Xu, L.Z. (2016). Irisin promotes osteoblast proliferation and differentiation via activating the MAP kinase signaling pathways. Sci. Rep. *6*, 1–12. https://doi.org/10.1038/SREP18732.

Rose, A.J., and Hargreaves, M. (2003). Exercise increases Ca2+-calmodulin-dependent protein kinase II activity in human skeletal muscle. J. Physiol. *553*, 303–309. https://doi.org/10.1113/JPHYSIOL.2003.054171.

Ruas, J.L., White, J.P., Rao, R.R., Kleiner, S., Brannan, K.T., Harrison, B.C., Greene, N.P., Wu, J., Estall, J.L., Irving, B.A., et al. (2012). A PGC-1α isoform induced by resistance training regulates skeletal muscle hypertrophy. Cell *151*, 1319–1331. https://doi.org/10.1016/J.CELL.2012.10.050.

Salminen, A., Braun, T., Buchberger, A., Jürs, S., Winter, B., and Arnold, H.H. (1991). Transcription of the muscle regulatory gene Myf4 is regulated by serum components, peptide growth factors and signaling pathways involving G proteins. J. Cell Biol. *115*, 905–917. https://doi.org/10.1083/JCB.115.4.905.

Samy, D.M., Ismail, C.A., and Nassra, R.A. (2015). Circulating irisin concentrations in rat models of thyroid dysfunction – effect of exercise. Metabolism *64*, 804–813. https://doi.org/10.1016/J.METABOL.2015.01.001.

Selsby, J.T., Morine, K.J., Pendrak, K., Barton, E.R., and Sweeney, H.L. (2012). Rescue of dystrophic skeletal muscle by PGC-1α involves a fast to slow fiber type shift in the mdx mouse. PLoS One *7*, e30063. https://doi.org/10.1371/JOURNAL.PONE.0030063.

Staron, R.S., Karapondo, D.L., Kraemer, W.J., Fry, A.C., Gordon, S.E., Falkel, J.E., Hagerman, F.C., and Hikida, R.S. (1994). Skeletal muscle adaptations during early phase of heavy-resistance training in men and women. J. Appl.

Physiol. *76*, 1247–1255. https://doi.org/10.1152/JAPPL.1994.76.3.1247.

Turner, N.J., Jones, H.S., Davies, J.E., and Canfield, A.E. (2008). Cyclic stretch-induced TGFbeta1/Smad signaling inhibits adipogenesis in umbilical cord progenitor cells. Biochem. Biophys. Res. Commun. *377*, 1147–1151. https://doi.org/10.1016/J.BBRC.2008.10.131.

Vandenburgh, H.H. (1982). Dynamic mechanical orientation of skeletal myofibers in vitro. Dev. Biol. *93*, 438–443. https://doi.org/10.1016/0012-1606(82)90131-2.

Vandenburgh, H.H., Hatfaludy, S., Karlisch, P., and Shansky, J. (1989). Skeletal muscle growth is stimulated by intermittent stretch-relaxation in tissue culture. Am. J. Physiol. *256*, C674–C682. https://doi.org/10.1152/AJPCELL.1989.256.3.C674.

Vandenburgh, H.H., and Karlisch, P. (1989). Longitudinal growth of skeletal myotubes in vitro in a new horizontal mechanical cell stimulator. In Vitro Cell. Dev. Biol. *25*, 607–616. https://doi.org/10.1007/BF02623630.

Yin, X., Mead, B.E., Safaee, H., Langer, R., Karp, J.M., and Levy, O. (2016). Engineering stem cell organoids. Cell Stem Cell *18*, 25–38. https://doi.org/10.1016/J.STEM.2015.12.005.

Zöllner, A.M., Abilez, O.J., Böl, M., and Kuhl, E. (2012). Stretching skeletal muscle: chronic muscle lengthening through sarcomerogenesis. PLoS One *7*, e45661. https://doi.org/10.1371/JOURNAL.PONE.0045661.

STAR★METHODS

KEY RESOURCES TABLE

REAGENT or RESOURCE	SOURCE	IDENTIFIER
Antibodies		
Anti-MyoD	Santa Cruz	Cat# SC-32758 RRID:AB_627978
Anti-Myogenin	Santa Cruz	Cat# SC-12732 RRID:AB_627980
Anti-Alkaline Phosphatase	Abcam	Cat# ab65834; RRID:AB_1139987
Anti-osteocalcin	Abcam	Cat# ab93876 RRID:AB_10675660
Anti-PGC-1a	Calbiochem	Cat# ST1202 RRID:AB_2237237
Alexa Fluor™ Plus 555 Phalloidin	Thermo Fisher	Cat#A30106
Anti-GAPDH	Abcam	Cat# ab181602 RRID:AB_2630358
Chemicals, peptides, and recombinant proteins		
DMEM/High glucose with L-glutamine	Hyclone	Cat# #30071.03
Alpha-MEM	Hyclone	N/A
Fetal Bovine Serum	Beyotime	Cat#C0231
Penicillin-Streptomycin	Hyclone	N/A
Horse Serum	Beyotime	N/A
TRizol Reagent	Ambion	Cat#207006
DAPI	HelixGen	N/A
Proteinase	Thermo Fisher	Cat#EO0491
Proteinase inhibitor cocktail	Abcam	Cat#ab270055
Phosphatase inhibitor	Cell Signaling	Cat#5870
BSA	Invitrogen (Thermo Fisher)	Cat#B14
4% Paraformaldehyde	Beyotime	N/A
Triton X-100	Beyotime	N/A
Critical commercial assays		
PrimeScript™ RT reagent kit	TaKaRa	Cat#RR037A
SYBR Premix Ex Taq kit	TaKaRa	Cat#RR820A
BCA kit	Beyotime	Cat#P0010S
Irisin ELISA kit	Phoenix Pharmaceuticals	Cat#EK06729; RRID:AB_2783013)
Lipofectamine™ 2000 Transfection Reagent	Thermo Fisher	Cat#11668027
Experimental models: Cell lines		
C2C12 myoblasts	National infrastructure of cell line resources (originally generated by YaffeD, SaxelO)	1101MOU-PUMC000099
$C2C12^{FNDC5-/-}$ myoblasts	In this paper	N/A
MC3T3-E1 osteoblasts	National infrastructure of cell line resources	1101MOU-PUMC000012

(*Continued on next page*)

Continued

REAGENT or RESOURCE	SOURCE	IDENTIFIER
Oligonucleotides		
Primer sequences: Runx2 forward primer 5′-CCAGCAGCACTCCATATC-3′	Designed on Primer3	NM_009,820
Primer sequences: Runx2 reverse primer 3′- ATCAGCGTCAACACCATC-5′	Designed on Primer3	NM_009,820
Primer sequences: Osx forward primer 5′-TGTCTCCTCAGTTCTTCTCT-3′	Designed on Primer3	NM_130458
Primer sequences: Osx reverse primer 5′-AGATTAGATGGCAACGAGTT-3′	Designed on Primer3	NM_130458
Primer sequences: Atf4 forward primer 5′-GATAGAAGAGGTCCGTAAGG-3′	Designed on Primer3	NM_009716
Primer sequences: Atf4 reverse primer 5′-AACACAGCAACACAAGACTA-3′	Designed on Primer3	NM_009716
Primer sequences: Alp forward primer 5′-CCGCAGGATGTGAACTAC-3′	Designed on Primer3	NM_007431
Primer sequences: Alp reverse primer 5′-GCCATCTTAGCAGCAACT-3′	Designed on Primer3	NM_007431
Primer sequences: Col1a1 forward primer 5′-ATCACCAGACGCAGAAGT-3′	Designed on Primer3	NM_007742
Primer sequences: Col1a1 reverse primer 5′-CTCATCATAGCCATAGGACAT-3′	Designed on Primer3	NM_007742
Primer sequences: Spp1 forward primer 5′-AATGCTGTGTCCTCTGAAG-3′	Designed on Primer3	NM_009263
Primer sequences: Spp1 reverse primer 5′-ATCGTCATCATCATCGTCAT-3′	Designed on Primer3	NM_009263
Primer sequences: Sost forward primer 5′-CCGTGTAGACTGGTGAGA-3′	Designed on Primer3	NM_024449
Primer sequences: Sost reverse primer 5′-TGGATTTGAAGGCAGATTTG-3′	Designed on Primer3	NM_024449
Primer sequences: MyoD forward primer 5′-CCGCAGGATGTGAACTAC-3′	Designed on Primer3	NM_010866
Primer sequences: MyoD reverse primer 5′-GCCATCTTAGCAGCAACT-3′	Designed on Primer3	NM_010866
Primer sequences: Myogenin forward primer 5′-ATCACCAGACGCAGAAGT-3′	Designed on Primer3	NM_031189.2
Primer sequences: Myogenin reverse primer 5′-CTCATCATAGCCATAGGACAT-3′	Designed on Primer3	NM_031189.2
Primer sequences: Desmin forward primer 5′-AATGCTGTGTCCTCTGAAG-3′	Designed on Primer3	NM_010043
Primer sequences: Desmin reverse primer 5′-ATCGTCATCATCATCGTCAT-3′	Designed on Primer3	NM_010043
Primer sequences: MyF5 forward primer 5′-CTCTGAAGGATGGACATGACGG-3′	Designed on Primer3	NM_008656
Primer sequences: MyF5 reverse primer 5′-ACTGGTCCCCAAACTCATCCTC-3′	Designed on Primer3	NM_008656
Primer sequences: PGC-1α1 forward primer 5′-ATCACCAGACGCAGAAGT-3′	Harvard PrimerBank	NM_008904
Primer sequences: PGC-1α1 reverse primer 5′-CTCATCATAGCCATAGGACAT-3′	Harvard PrimerBank	NM_008904

(*Continued on next page*)

Continued

REAGENT or RESOURCE	SOURCE	IDENTIFIER
Primer sequences: PGC-1α2 forward primer 5′-AATGCTGTGTCCTCTGAAG-3′	Ruas et al., (2012)	N/A
Primer sequences: PGC-1α2 reverse primer 5′-ATCGTCATCATCATCGTCAT-3′	Ruas et al., (2012)	N/A
Primer sequences: PGC-1α3 forward primer 5′-CCGTGTAGACTGGTGAGA-3′	Ruas et al., (2012)	N/A
Primer sequences: PGC-1α3 reverse primer 5′-TGGATTTGAAGGCAGATTTG-3′	Ruas et al., (2012)	N/A
Primer sequences: PGC-1α4 forward primer 5′-CCGTGTAGACTGGTGAGA-3′	Ruas et al., (2012)	N/A
Primer sequences: PGC-1α4 reverse primer 5′-TGGATTTGAAGGCAGATTTG-3′	Ruas et al., (2012)	N/A
Primer sequences: GAPDH forward primer 5′-CCGTGTAGACTGGTGAGA-3′	Designed on Primer3	NM_001289726
Primer sequences: GAPDH reverse primer 5′- TGGATTTGAAGGCAGATTTG-3′	Designed on Primer3	NM_001289726
PGC-1α1siRNA 5′-CCGCAAUUCUCCCUUGUAUTT-3′	In this paper	N/A
PGC-1α4siRNA 5′-GCGACCAAUCGGAAAUCAUTT-3′	In this paper	N/A
Software and algorithms		
FlexSoft® FX-5000™ Software	Flexcell home	N/A
ImageJ	https://imagej.nih.gov/ij/	RRID:SCR_003070
GraphPad Prism Version 6	https://www.graphpad.com/	RRID:SCR_015807
SnapGene	http://www.snapgene.com/	RRID:SCR_015052
Other		
24 mm Transwell® with 0.4 μm Pore Polyester Membrane Insert	Corning	Cat#3450
Transwell holder for 6-well plate	Flexcell	N/A
BioFlex 6-well plate	Flexcell	N/A
FX-5000T™ Tension System	Flexcell	FX-5000T
BioFlex® Culture Plates	Flexcell	Cat#BF3001
FX-5000T™ Flexlink® Controller	Flexcell	FX-5000T

RESOURCE AVAILABILITY

Lead contact

Further information and requests for resources and reagents should be directed to and will be fulfilled by the lead contact, Lizhen Wang (lizhenwang@buaa.edu.cn).

Materials availability

The new cell line C2C12$^{FNDC5-/-}$ (homozygous FNDC5 gene knocked out myoblast) generated in this study are available from the lead contact and recourses information have been listed in the key resources table and the generation of this cell line is described in this paper.

Data and code availability

Data reported in this paper will be shared by the lead contact upon request. This paper does not report original code. Any additional information required to reanalyze the data reported in this paper is available from the lead contact upon request.

EXPERIMENTAL MODEL AND SUBJECT DETAILS

Cell culture, co-culture & differentiation

C2C12 myoblasts were seeded on the silicone membrane on BioFlex 6-well plate and cultured in proliferation media with 90% DMEM, 10% fetal bovine serum and 1% penicillin-streptomycin at 37.0°C for 2 days when they reached ~90% confluence, followed by 6 days of Differentiation media with 90% DMEM, 2% horse serum and 1% penicillin-streptomycin. MC3T3-E1 cells were plated on the transwell and incubated with 90% alpha-MEM, 10% fetal bovine serum and 1% penicillin-streptomycin at 37.0°C for 2 days to proliferate. When cells reached to 100% confluence, the transwell with cells was immediately transfer on a holder supported on the BioFlex 6-well plate with differentiated myotubes on bottom. Co-culture system with MC3T3 cells and myotubes was mounted on a loading platform (Flexcell, USA) and connected the system vacuum to the SYSTEM port on the back of the FlexLink® (Flexcell, USA). FlexLink® and computer system were turned on to start the vacuuming to stretch the membrane. Cyclic strain parameters were set in the software (FX- 5000TM icon, USA). Culturing atmosphere contained 95% air and 5% CO_2, which guaranteed cells normal growth. The co-culture media was renewed every 24 h.

METHOD DETAILS

Cyclic stretch stimulated irisin determination

Myoblasts samples were homogenized using 20g syringe and needle in lysis buffer including 100 mM Tris, 150 mM NaCl, 1 mM EGTA, 1 mM EDTA, 1% Triton X-100, protease and phosphatase inhibitors. Measure DNA concentration using nanodrop, calculate the total DNA content in each sample.

Pipette cell culture media, supplemented with protease and phosphatase inhibitors into a prechilled centrifuge tube and centrifuge at 1,500 rpm for 10 min at 4°C. Aliquot supernatant immediately and store samples at −80 °C. Irisin levels were measured from cell supernatants with Phoenix Pharmaceuticals ELISA kit directed against full-length recombinant irisin and antibody directed against FNDC5 residues 42–112 according to manufacturer's instructions. Irisin concentration of each sample was normalized with the DNA concentration of the corresponding irisin-inducing myoblasts in each niche.

RNA interfering

2 distinct siRNA were designed, termed siPGC-1α1 and siPGC-1α4 (sense sequence can be found in Key recourses table). Due to an overlapped region existed on both mRNA transcripts, among which the PGC-1α1 transcript, the longer one, carries an additional region than PGC-1α4. Thus, siPGC-1α1s was designed to specifically target on its additional arm. Consequently, siPGC-1α4 was able to non-specifically interfere the interfere PGC-1α4 mRNA, what's more, equivalent regions on PGC-1α1 mRNA (Figure 4D). 100pmol siRNA and 5ul of lipofectamine was diluted in 250ul serum reduced and antibiotics free media separately and incubated for 5 min at RT (one well in 6-well plate). Mix siRNA and lipofectamine gently, 500ul of complexes was added into each well containing ells and medium. Mix gently by rocking the plate back and forth. Incubate cells at 37 °C in a CO2 incubator for 48 h prior to testing for transgene expression.

RNA isolation and real-time PCR

qPCR was implemented after the Total RNA extraction, which was collected by TRizol Reagent according to the manufacturer's introduction. PrimeScript™ RT reagent kit was subject to reverse transcription of the RNA samples to cDNA. Afterwards, by using SYBR Premix Ex Taq kit and following its instruction, the quantitative PCR results were obtained on an iCycler iQ5 Cromo4 (Bio-Rad, USA). Mouse GAPDH was performed to normalize cDNA. The relative expression results were calculated using the $2^{-\Delta\Delta ct}$ method. Primers of relative genes for Real-time PCR were provided in Key recourses table.

Western blotting

Cells were lysed in the lysis buffer. Total protein was extracted to the supernatant, collected for the following Western blot assay. Subsequently, the BCA kit was developed to detect protein concentration, while 50 μg proteins were added to each SDS-PAGE gel. All the protein blots were transferred to nitrocellulose membranes (Millipore, USA), followed by blocking with 5% skim milk. The target protein including MyoD, Myogenin, PGC-1α, Alp, Col1α1 and Ocn were incubated respectively by primary antibodies including Anti-MyoD (1:1000), Anti-Myogenin (1:1000), Anti-Alkaline Phosphatase (1:1000) and Anti-osteocalcin (1:1000), and were identified by further incubation with goat anti-rabbit IgG H&L as

second antibodies (1:10,000). To detect all PGC-1a variants by immunoblotting, anti-PGC-1a antibodies were obtained from Calbiochem. The eventual results were visualized by using ChemiDocXRS (Bio-Rad, USA) and ImageJ software. All antibodies employed in this study can be found in the Key recourses table.

Immunofluorescence staining

We applied the Immunofluorescent assay to visualize the monophony of nascent and multinuclear myotubes. Differentiated myotubes grown on flexible membrane were fixed by 4%paraformaldehyde, followed by permeabilization with 0.1%Triton X-100 and blocking with 5%BSA to diminish the background fluorescence. F-actin was stained directly with 1:200 TRITC-conjugated phalloidin (1: 1000), counterstained and mounted with DAPI (1:1000), the cells were observed and photographed by laser scanning confocal microscope (Leica Microsystems, Germany).

QUANTIFICATION AND STATISTICAL ANALYSIS

All variables in the data were presented as mean $\pm$ standard error of mean. Every single test was repeated for three times. At first, the two-tailed Student's *t* test was applied to the comparisons between two variables. Then, we performed the One-Way ANOVA to verify comparisons among three repeated groups, two-way ANOVA with Tukey's or Dunnett's tests were used for datasets with a normal distribution. For all tests, $p < 0.01$ was considered to be statistically significant.